

RF MEMS Oscillator with Integrated Resistive Transduction

R. B. Reichenbach, M. Zalalutdinov, J. M. Parpia, and H. G. Craighead

Abstract—A method to integrate micromechanical frequency-determining elements along with the corresponding electro-mechanical transducers into a poly or single-crystal silicon film layer is demonstrated. A resistor dissipating several microwatt of power induces high-frequency resonant mechanical motion in a shallow-shell membrane. Transduction from the mechanical to the electrical domain is performed using implanted piezoresistors, which are sensitive to strain produced by resonant motion. Self-sustained oscillations at 10 MHz are demonstrated when the device is directly coupled to a high-impedance operational amplifier and a positive feedback loop. Finally, this letter discusses how the resonator and transducers may be incorporated into standard integrated-circuit technology.

Index Terms—CMOS integrated circuits, microelectromechanical devices, oscillators, resistance heating, resonators.

I. INTRODUCTION

HIGH-FREQUENCY microelectromechanical systems (MEMS) resonators have demonstrated outstanding performance as frequency-determining elements for communication systems. Featuring quality (Q) factors of $Q \sim 10\,000$ and occupying chip real estate less than $100 \times 100 \mu\text{m}^2$, micromechanical devices are capable of revolutionizing radio frequency (RF) signal processing by replacing offchip components with MEMS filters [1]–[3], oscillators [4]–[6], and mixers [7], [8]. Microminiaturized mechanical components offer significant advantages over macroscaled electrical components in terms of linearity, cost, size, and power consumption [9]; however, they suffer from the need for highly specialized fabrication steps to realize their physical form. Critically defined gaps [4], novel materials [1], [10], and nonplanar geometries [11] represent significant barriers for integrating micromechanical resonant structures and their transduction elements into a CMOS environment.

In this letter, we present a high-frequency shell-type micromechanical resonator (Fig. 1) with an integrated electrical–mechanical transduction. Mechanical motion of a polysilicon thin-film plate or shell-type resonator is produced by the effects of heat transferred from a resistive microheater. Detection of the resonant motion is enabled through an im-

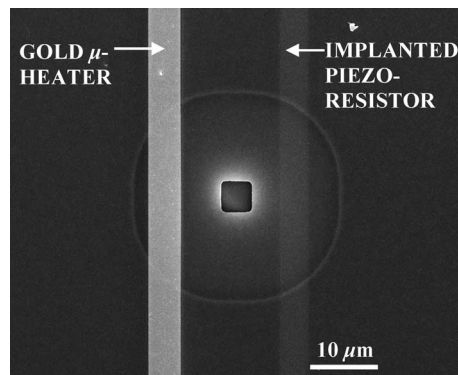


Fig. 1. SEM image of a shell-type RF MEMS resonator with integrated resistive transducers. The white outer ring defines the circumference of the membrane. A 30-nm-thick metal resistor and an implanted p-type resistor form the input/output transducers. Image obtained using a mix of inlens secondary detector and inlens energy selective backscatter detector on a Carl Zeiss Ultra 55.

planted piezoresistive active region in the suspended structure. Thus, microresistors couple energy into and out of the microresonator. Resistive coupling offers several advantages over electrostatic transduction: The actuators are broadband and can be impedance matched to the network, their performance does not depend on nanometer scaled gaps surrounding the resonator, and the impact on the resonator Q factor is minimized. Finally, both resistive transducers can be fabricated within the polysilicon membrane, allowing a resonator to be implemented into a single plane of silicon and defined immediately next to a field-effect transistor in a CMOS process.

II. FABRICATION

Fig. 2(a) illustrates the cross-sectional view of the micromechanical resonator and thermal transducer. A sacrificial layer of SiO_2 , which is followed by an LPCVD polysilicon film, is deposited on a silicon substrate. Etch holes are patterned into the device layer using photolithography and a subsequent CF_4 RIE etch. A second layer of photolithography defines the areas of the polysilicon that will be doped to form the piezoresistive strip. The $70 \times 3 \mu\text{m}$ area of implantation is positioned in the membrane to be sensitive to modes such as γ_{01} and γ_{11} , described in [12]. Using the thick resist as a mask, the film stack is subjected to boron ion implantation at a dose of $5 \times 10^{15} \text{ cm}^{-2}$ and energy of 5 keV. The resulting shallow implant creates an asymmetrical piezoresistive region through the polysilicon film thickness. Subsequent rapid thermal annealing at $900 \text{ }^\circ\text{C}$ for 30 s activates the boron and limits diffusion of the active species. Following implantation and activation, the chip is

Manuscript received April 18, 2006; revised July 11, 2006. The review of this letter was arranged by Editor J. Sin.

R. B. Reichenbach is with the Department of Electrical and Computer Engineering, Cornell University, Ithaca, NY 14853 USA (e-mail: rbr9@cornell.edu).

M. Zalalutdinov and J. M. Parpia are with the Department of Physics, Cornell University, Ithaca, NY 14853 USA.

H. G. Craighead is with the Department of Applied and Engineering Physics, Cornell University, Ithaca, NY 14853 USA.

Digital Object Identifier 10.1109/LED.2006.882526

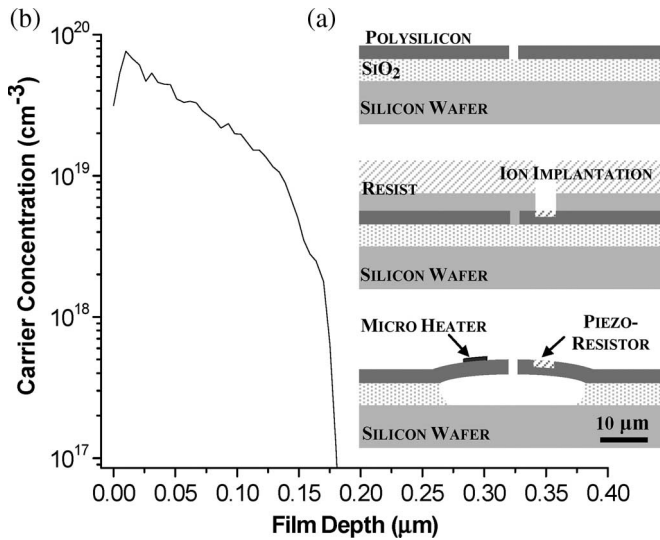


Fig. 2. (a) Cross-sectional view of resonator and transducer fabrication process. The gold microheater could be implemented as a second implanted resistor to realize a completely integrated resonator and transducer. (b) Spreading resistance profile of active boron concentration in the implanted piezoresistor.

placed in an HF bath to undercut the polysilicon and define the radius of the resonator. A spreading resistance profile [Fig. 2(b)] shows active boron concentration varying between 1×10^{20} and $1 \times 10^{17} \text{ cm}^{-3}$ through the 180-nm polysilicon film. Due to the asymmetric profile, transverse vibrations, characterized by expansion in the top half and compression in the bottom half of the film, will produce a change in the resistance along the length of the piezoresistor. In contrast, a film with uniform doping, through its thickness, would provide no net change in resistance from flexure. Since the gauge factor of polysilicon varies with doping concentration, the difference in the gauge factor between the top and bottom sections of the film determines the overall sensitivity to membrane stress. The thermal mechanical actuator could be created in a similar method; however, we follow previous research [7], [13] and define a thin-film metal resistor on the surface of the micromechanical resonator. The $70 \times 3 \mu\text{m}$ metal microheater is configured to present a $50\text{-}\Omega$ match to the input electronics, minimizing signal reflection. The location of the metal strip impacts damping in the mechanical system through electron-phonon interactions in the metallic film, in this geometry reducing the Q factor by approximately 30%. However, sufficient drive forces are still obtained, and Q degradation is prevented when the resistor is located adjacent to the membrane.

III. RESULTS AND DISCUSSION

Mechanical motion in the microresonator is produced by applying a -20-dBm RF signal and 250-mV dc bias to the microheater (Fig. 3). Joule heat is dissipated by the resistor directly into the thin-film membrane, producing thermal expansion and subsequent out-of-plane deflection in the resonator. The short thermal diffusion time constants of the polysilicon microresonator enable high modulation rates. When the frequency of the RF signal matches the natural resonant fre-

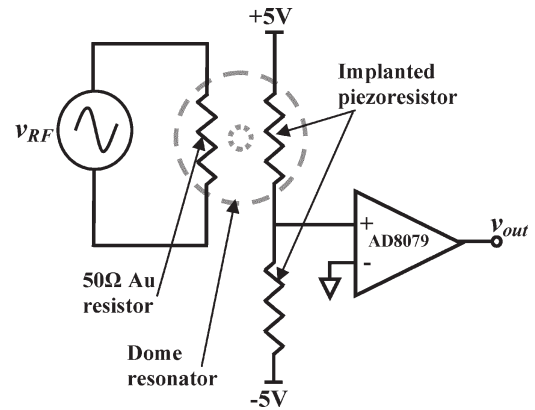


Fig. 3. Electrical signal path through the MEMS resonator with resistive transduction.

quency of the membrane, standing waves are excited in the structure [12].

The implanted polysilicon resistor monitors the high displacement $Q = 5000$ to $15\,000$ (depending on the mode of vibration) resonant motion [14], [15]. Membrane deflection produces a corresponding strain in the shell membrane, which is converted by the piezoresistive effect in the doped polysilicon strip into a proportional fractional change in resistance. In a half-Wheatstone bridge configuration, a change in resistance in one of the two resistors will produce corresponding voltage variations at the center of the bridge. Strain developed in the resonator along the piezoresistive strip is on the order of 10^{-5} , which, for a differential gauge factor of ~ 10 , a bridge bias of 10 V , and resistor value of $4 \text{ k}\Omega$, would produce an ac output signal of about 1 mV .

Initial resonator testing was performed using a Desert Cryogenics vacuum probe station. The half bridge was biased with $\pm 5 \text{ V}$, and a third probe connected the middle of the bridge to the $50\text{-}\Omega$ input of a spectrum analyzer. The output spectrum of this configuration is shown in Fig. 4(a) and (b). In the polar plot of Fig. 4(b), the peak of the resonance has a magnitude of $10 \mu\text{V}$ and is offset from the origin due to coupling (crosstalk) between the drive and detection. Crosstalk was found to be on the order of -80 dB and primarily dominated by capacitive coupling rather than thermal coupling within the resonator membrane.

A high-impedance buffer amplifier placed directly on the piezoresistive bridge output serves to reduce voltage division between the implanted resistors and spectrum analyzer input as well as eliminate parasitic capacitances associated with probes and cabling. We chose an analog devices AD8079 high-speed buffer with a gain of two, which presents a $10 \text{ M}\Omega$ and 1.5 pF input resistance and capacitance, respectively. Fig. 4(c) displays the Lorentzian waveform produced by the same resonator and -20-dBm RF drive, only now wirebonded to an amplifier prototyping board. Inband insertion loss is reduced from -65 to -35 dB ; however, out-of-band attenuation is partially compromised due to coupling between the unshielded gold ribbon wire bonds. Optimizing the fabrication parameters and location of the resistive transducers will significantly reduce conversion loss in the MEMS system.

Detection of motion at the frequency of vibration, as opposed to heterodyne detection [16], allows the resonator to lock onto

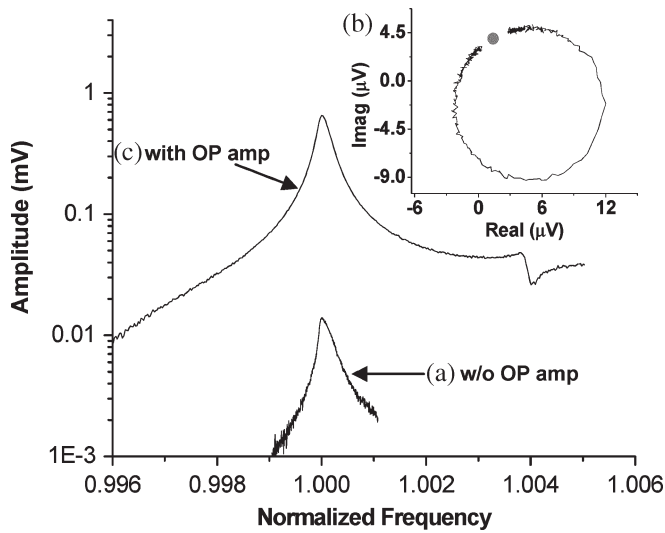


Fig. 4. Lorentzian response of one membrane mode excited and detected by the resistive transducers both (a and b) uncoupled and (c) coupled to an operational amplifier. The background crosstalk vector in (a) is indicated by the gray dot in (b). The background vector has been subtracted from both (a) and (c). Microheater drive signal is -20 dBm with a 250-mV bias and 10-V piezoresistor bridge bias.

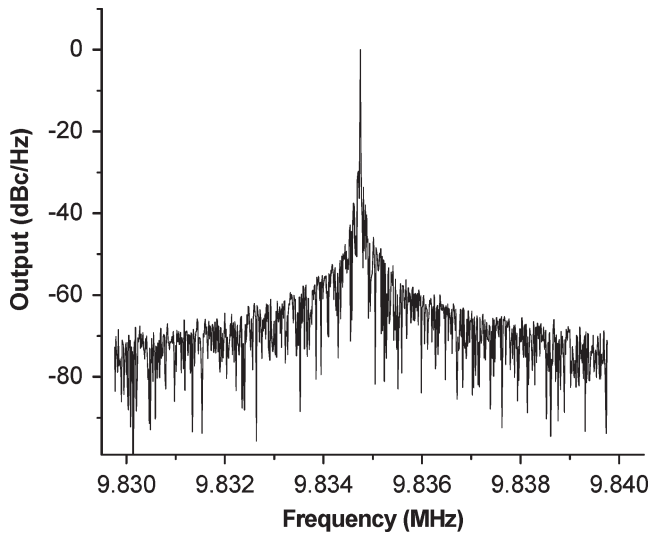


Fig. 5. MEMS Oscillator spectrum sampled after the tuned feedback amplifier.

its own mechanical motion via a feedback loop. Feedback is provided outside the vacuum chamber by means of a MATEC tuned receiver, allowing control of loop phase and amplitude. Mechanical oscillation at 9.8 MHz was achieved with approximately 20 dB of loop gain (not including the preamplifier gain) and is pictured in Fig. 5. The noise floor was determined by the feedback loop, preventing phase noise measurements of the MEMS oscillator.

IV. CONCLUSION

We demonstrate a method where both the mechanical frequency-determining element and the transduction elements

can be incorporated into a single device layer. IC layouts typically have a polysilicon gate/resistor layer, which can be selectively doped and is surrounded by an isolation oxide. Removing the oxide would create a suspended polysilicon membrane with integrated implanted transducers, whose performance would be independent of the surrounding air gap. Such an implementation, along with onchip buffer amplifiers, would significantly reduce capacitive crosstalk effects in the resonator, enabling high performance measurements and facilitating the incorporation of micromechanical frequency determining components into a standard RFIC fabrication processes.

REFERENCES

- [1] H. Chandralahim, D. Weinstein, L. F. Cheow, and S. A. Bhavé, "Channel-select micromechanical filters using high- k dielectrically transduced MEMS resonators," in *Proc. 19th IEEE Int. Conf. MEMS*, Istanbul, Turkey, Jan. 22–26, 2006, pp. 894–897.
- [2] M. U. Demirci and C. T.-C. Nguyen, "A low impedance VHF micromechanical filter using coupled-array composite resonators," in *Proc. 13th Int. Conf. Solid-State Sens. & Actuators (Transducers)*, Seoul, Korea, Jun. 5–9, 2005, pp. 2131–2134.
- [3] M. Zalalutdinov, J. W. Baldwin, M. H. Marcus, R. B. Reichenbach, J. M. Parpia, and B. Houston, "Two-dimensional array of coupled nanomechanical resonators," *Appl. Phys. Lett.*, vol. 88, no. 14, p. 143504, Apr. 2006.
- [4] V. Kaajakari, T. Mattila, A. Oja, J. Kiihamäki, and H. Seppä, "Square-extensional mode single-crystal silicon micromechanical resonator for low phase noise oscillator applications," *IEEE Electron Device Lett.*, vol. 25, no. 4, pp. 1486–1503, Aug. 1999.
- [5] Y. Xie, S.-S. Li, Y.-W. Lin, Z. Ren, and C. T.-C. Nguyen, "UHF micromechanical extensional wine-glass mode ring resonators," in *IEDM Tech. Dig.*, Washington, DC, Dec. 8–10, 2003, pp. 953–956.
- [6] R. B. Reichenbach, K. L. Aubin, M. Zalalutdinov, J. M. Parpia, and H. G. Craighead, "A MEMS RF phase and frequency modulator," in *Proc. 13th Int. Conf. Solid-State Sens. & Actuators (Transducers)*, Seoul, Korea, Jun. 5–9, 2005, pp. 1059–1062.
- [7] R. B. Reichenbach, M. Zalalutdinov, K. L. Aubin, R. Rand, B. Houston, J. M. Parpia, and H. G. Craighead, "3rd Order Intermodulation in a Micromechanical Thermal Mixer," *J. Microelectromech. Syst.*, vol. 14, no. 6, pp. 1244–1252, Dec. 2005.
- [8] A.-C. Wong and C. T.-C. Nguyen, "Micromechanical mixer-filters ("mixlers")," *J. Microelectromech. Syst.*, vol. 13, no. 1, pp. 100–112, Feb. 2004.
- [9] C. T.-C. Nguyen, "Microelectromechanical devices for wireless communications," in *Proc. 11th Annu. Workshop Micro Electro Mech. Syst.*, Jan. 25–29, 1998, pp. 1–7.
- [10] R. C. Ruby, A. Barfknecht, C. Han, Y. Desai, F. Geefay, G. Gan, M. Gat, and T. Verhoeven, "High- Q FBAR filters in a wafer-level chip-scale package," *IEEE Int. Solid-State Circuits*, vol. 35, no. 4, pp. 512–526, Apr. 2000.
- [11] J. R. Clark, W.-T. Hsu, M. A. Abdelmoneum, and C. T.-C. Nguyen, "High- Q UHF micromechanical radial-contour mode disk resonators," *J. Microelectromech. Syst.*, vol. 14, no. 6, pp. 1298–1310, Dec. 2005.
- [12] M. Zalalutdinov, K. L. Aubin, C. Michael, R. B. Reichenbach, T. Alan, A. T. Zehnder, B. H. Houston, J. M. Parpia, and H. G. Craighead, "Shell-type micromechanical oscillator," *Proc. SPIE*, vol. 5116, pp. 229–236, 2003.
- [13] M. Zalalutdinov, K. L. Aubin, R. B. Reichenbach, A. T. Zehnder, B. Houston, J. M. Parpia, and H. G. Craighead, "Shell-type micromechanical actuator and resonator," *Appl. Phys. Lett.*, vol. 83, no. 18, pp. 3815–3817, Nov. 2003.
- [14] R. P. Ried, H. J. Mamin, B. D. Terris, L. S. Fan, and D. Rugar, "5 Mhz, 2 N/m piezoresistive cantilevers with incisive tips," in *Proc. Int. Conf. Solid-State Sens. & Actuators (Transducers)*, Chicago, IL, Jun. 16–19, 1997, pp. 447–550.
- [15] Y. A. Liang, S. W. Ueng, and T. W. Kenny, "Performance characterization of ultra-thin n-type piezoresistive cantilevers," in *Proc. Solid-State Sens. and Actuators Conf.*, 2001, pp. 998–1001.
- [16] I. Bargatin, E. B. Myers, J. Arlett, B. Gudlewski, and M. L. Roukes, "Sensitive detection of nanomechanical motion using piezoresistive signal downmixing," *Appl. Phys. Lett.*, vol. 86, no. 13, p. 133109, Mar. 2005.